

## STOCHASTIC DYNAMIC RESPONSE OF A CROSS ROPE TRANSMISSION LINE

**Bruno J. Rango<sup>a</sup>, Marta B. Rosales<sup>b</sup>, Jorge S. Ballaben<sup>a</sup>, Roberta Lima<sup>c</sup> and Rubens Sampaio<sup>c</sup>**

<sup>a</sup>*Department of Engineering, Universidad Nacional del Sur, Alem 1253, 8000 Bahía Blanca and CONICET, Argentina, brunorango@gmail.com, jorgeballaben@gmail.com*

<sup>b</sup>*Department of Engineering, Universidad Nacional del Sur, Alem 1253, 8000 Bahía Blanca and IFISUR (UNS-CONICET), Argentina, mrosales@criba.edu.ar*

<sup>c</sup>*Mechanical Engineering Department, PUC-Rio, Rio de Janeiro, RJ, Brazil, robertalima@puc-rio.br, rsampaio@puc-rio.br*

**Keywords:** Transmission lines, Cross rope tower, stochastic wind load

**Abstract.** Cross Rope (CR) structures are increasingly used in High Voltage (HV) and Ultra High Voltage (UHV) transmission lines (TLs). The configuration of this kind of structures consists of two steel truss masts, each of which is grounded by two guy-cables connected at their upper end. The masts present no rigid connection between them: they are only linked by the CR cable which, likewise, supports the insulator chains and therefore the conductors. The implementation of this structural typology in transmission lines is relatively recent and its popularity is rising due to some favorable features when compared to self-supporting towers and other configurations of guyed structures (their low weight and associated low cost stand out). However, despite the recent application of CR structures in power lines around the world – Argentina, Brasil, South Africa, Australia, Canada – many aspects of their response to time-varying excitations have not been studied and documented in detail yet. In this work, a segment of a CR transmission line under stochastic wind load is addressed. The mathematical model for the dynamics of the different main structural elements (tower, insulators and cables) is stated, and the governing differential equations are discretized through the Finite Element Method. For the generation of the spatially and temporally correlated wind load field, the Spectral Representation Method (SRM) is applied. Attention is focused on the effect of the aerodynamic damping on the structural response.

## 1 INTRODUCTION

Cross Rope (CR) suspension structures are increasingly used in overhead power transmission systems. In effect, the most recent Extra High Voltage Transmission Lines constructed in Argentina implement CR as supporting towers. Their structural configuration (Fig. 1a) consists on the combination of two very efficient structural elements: cables in tension and lattices in compression. The two main lattice towers are guyed from their upper end through two wires.

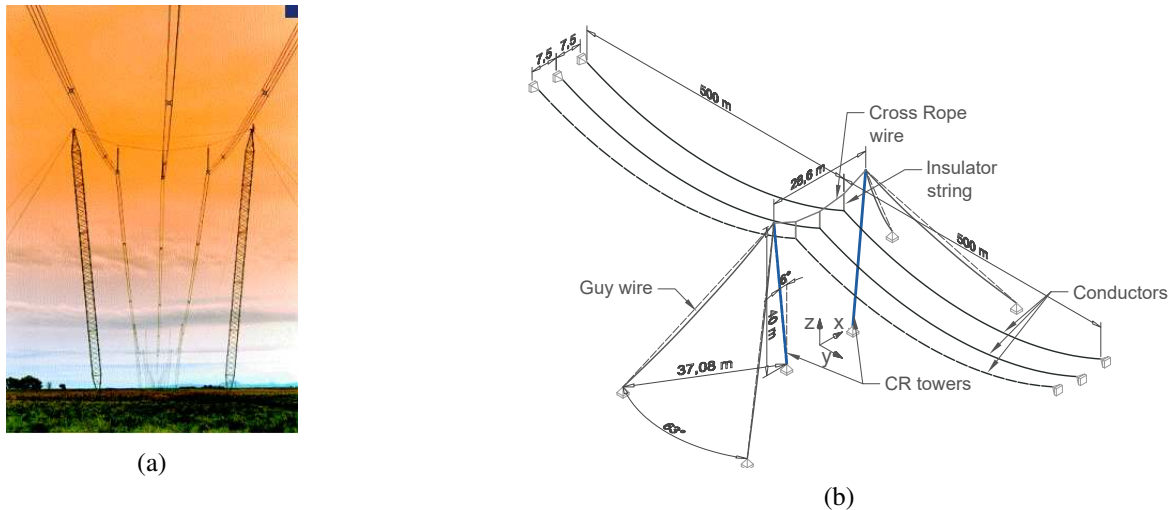


Figure 1: (a) Photograph of a transmission guyed tower of suspension-type. (b) Scheme of the simplified model of the guyed transmission line segment under study.

Likewise, lattices are connected to each other from their upper end through a transverse wire which gives name to the structural configuration: the Cross Rope. The lack of rigid connection between both towers is not the only singularity of this configuration. In fact, the insulator chains (which support the conductor cables) are not connected directly to lattices. Instead, they are linked to the supporting structure at the CR.

Besides low cost, there are additional reasons for which this particular structural configuration is selected instead of self-supported or other guyed-like structures: simple manufacturing and installation procedure, remarkable strength-to-weight ratio, low visual impact, reduced phase spacing (which results in a lower expropriation area along the line). On the other side, this kind of structures are flexible, their stability is strongly dependent on the tension of the guy cables, and their overall behavior is nonlinear. Moreover, the most demanding load is represented by wind, which is random in nature. As a result, the response of the transmission line to the load is random as well.

The literature devoted to the evaluation of transmission lines subjected to wind loads is vast. [Gani and Legeron \(2010\)](#), for instance, considers a single-mast guyed suspension tower and two adjacent conductor spans under stochastic wind load. The article is oriented towards the evaluation of the static-equivalent wind load proposed in the international standard [IEC 60826](#). They conclude that the static-equivalent method not always provides conservative results. Similarly, [Fleck Fadel Miguel et al. \(2012\)](#) performs a comparison of the outcomes from the application of the IEC recommended static load and a correlated stochastic wind load field, in this case to a self-supported transmission line, concluding that, if a detailed description of the structural behavior is sought, then a full dynamic analysis is to be performed. Moreover, the authors remark

on the importance of including model and structural uncertainties into the analysis. A different approach is adopted by Hamada et al. (2017): they construct a reduced-scale model consisting of four single-mast guyed suspension tower and the respective adjacent conductor spans. The structural features and dynamic response of the aeroelastic model subjected to wind fields of different mean velocity, generated in a boundary layer wind-tunnel, are evaluated. The study confirms that the dynamic behavior of the towers is dependent on the pretension level of the guys. Moreover, the authors conclude that the structure responds in a quasi-static manner to synoptic wind loads.

The present study addresses the uncovered evaluation of the dynamic response of a CR transmission line, subjected to stochastic wind field. The turbulent component of the wind speed is assumed to be characterized by the spectrum proposed by Davenport (1961). The spatial and temporal correlations of this component are accounted for. The stochastic, temporal, wind speed field for the wind load is generated by means of the Spectral Representation Method (SRM) (Shinozuka and Jan, 1972). The aerodynamic damping of the conductors is included in the model, in the form of resistive force proportional to the difference in speed between the conductor and the wind.

A mathematical model of a CR transmission tower and two adjacent spans of conductors in the 3D space is stated. The cable elements (*i.e.* guy wires, insulator strings, and conductors) are modeled according to the nonlinear formulation proposed by Luongo et al. (1984). The lattice tower, on the other side, is simplified as an equivalent column assuming the Euler-Bernoulli linear beam theory. The coupled nonlinear system of equations is discretized through the Finite Element Method.

A parametric sweep is performed: the reference mean wind speed characterizing the wind load field is varied. The along wind transient displacements at the center of one conductor cable and at the top of the leeward CR tower is analyzed. The ergodic property of those stochastic processes is used in order to derive statistics from single realizations. Indeed, the temporal mean and standard deviation are studied through the construction of envelope graphs. The effect of the aerodynamic damping is discussed.

## 2 DETERMINISTIC MATHEMATICAL MODEL

A scheme of the transmission line model under study is represented in Fig. 1b. Both supporting towers are alike: they consist of latticed towers of 40.20 m length inclined  $6^\circ$  with respect to the direction of the global z-axis (see Fig. 1b). Each mast is connected to ground from their upper support by two pre-stressed guy-wires and by their lower through a pinned ground connection. At they same time, the masts are connected to each other through the transverse CR. Three insulator chains of 4.5 m length hung from the transverse CR. Two adjacent conductor spans of 500 m are considered for the analysis. The conductors, which are connected from one end to the insulator strings and assumed pinned on their further end, display an initial sag of 22 m at the center of the span.

A mathematical model in the 3D-space is stated. Both latticed towers are modeled as equivalent beam-columns assuming the hypothesis of the Euler-Bernoulli beam theory for the bending problem. The formulas for the calculation of the equivalent properties were kindly provided by Dr. Marcelo Guzman, and constitute the extension to square cross-section towers of the equivalence formulas developed for towers of triangular section (Guzmán et al., 2017). Moreover, the axial and torsional deformations of the beam are considered, and the stress-strain relations are assumed linear. On the other side, the conductors, guy wires, CR, and insulator strings are modeled as elastic unidimensional cables, by means of the nonlinear formulation proposed by

Luongo et al. (1984). In this scheme, the following hypothesis are adopted: (i) the stress-strain relation is assumed linear, (ii) the flexural, torsional, and shear rigidities are neglected, (iii) the axial deformations of the cable are described through the Lagrangian strain measure, and (iv) the static equilibrium configuration is represented by a parabolic profile. This assumption is valid for taut cables, where the sag to span ratio is less or equal than 1/10, which is the case of all the cables in this work. The displacements of the cable during its motion are referred to the initial parabolic profile. The differential equations governing the beam-columns (subscript  $b$ ) and cable (subscript  $c$ ) dynamics are:

$$\begin{aligned}
 u_b &: m_b \ddot{u}_b + c_b \dot{u}_b - ea_b u_b'' = q_{u_b}(t, x_b) \\
 v_b &: m_b \ddot{v}_b + c_b \dot{v}_b + ei_z v_b'''' - nv_b'' = q_{v_b}(t, x_b) \\
 w_b &: m_b \ddot{w}_b + c_b \dot{w}_b + ei_y w_b'''' - nw_b'' = q_{w_b}(t, x_b) \\
 u_c &: m_c \ddot{u}_c + c_c \dot{u}_c - ea_c \varepsilon' = q_{u_c}(t, x_c) \\
 v_c &: m_c \ddot{v}_c + c_c \dot{v}_c - [hv_c' + ea_c(y' + v')\varepsilon]' = q_{v_c}(t, x_c) \\
 w_c &: m_c \ddot{w}_c + c_c \dot{w}_c - [hw_c' + ea_c w_c' \varepsilon]' = q_{w_c}(t, x_c)
 \end{aligned} \tag{1}$$

plus the corresponding boundary conditions. The displacements along the local  $\{x_{b,c}, y_{b,c}, z_{b,c}\}$  directions are  $\{u_{b,c}, v_{b,c}, w_{b,c}\}$ , and  $\theta_x$  is the twist angle of the beam around its longitudinal ( $x_b$ ) axis. The overdot ( $\dot{\cdot}$ ) stands for time derivative ( $d/dt$ ) and prime ( $\cdot$ )' denotes the space derivative ( $d/dx$ ). The external distributed forces acting on the cables in the axial and transverse directions are identified as  $q_{u_c}$  and  $q_{v_c}, q_{w_c}$ , respectively, whereas for the beam-columns those components are  $q_{u_b}$  and  $q_{v_b}, q_{w_b}$ . Likewise,  $m_{c,b}, c_{c,b}, ea_{c,b}$ , stand for the mass per unit length, damping, and axial stiffness of the cable and beam-columns, respectively. The torsional stiffness of the beam-columns is denoted  $gi_x$ , whereas  $ei_z$  and  $ei_y$  represent their bending stiffness with respect to the transverse local directions. The elongation of the cable is expressed by  $\varepsilon = u_c' + y_c' v_c' + 1/2(v_c'^2 + w_c'^2)$ , and  $y_c = 4d[x_c/l_c - (x_c/l_c)^2]$  is the equation of the parabola which describes the initial configuration of static equilibrium under self weight. The parameter  $h$  represents the static tension force acting on the cable. The geometric and mechanical properties considered for the study are reported in Tables 1 and 2. For details on the derivation of the governing differential equations, refer to Ballaben and Rosales (2018).

In the path towards the finite element discretization, the derivation of the weak form of the system governing equations constitutes the next step. For a detailed description of this process, please refer to Ballaben and Rosales (2018).

	$ea_b$ [N]	$ei_y$ [Nm <sup>2</sup> ]	$ei_z$ [Nm <sup>2</sup> ]	$gi_x$ [Nm <sup>2</sup> ]	$m_b$ [kg/m]	$\rho i_x$ [kgm]
Towers	$1.3276 \times 10^9$	$5.9240 \times 10^8$	$5.9240 \times 10^8$	$3.7797 \times 10^7$	67.84	56.39

Table 1: Geometrical and mechanical properties of the lattice towers modeled as an equivalent beam-columns.

## 2.1 Finite Element Discretization

After deriving the weak form of the governing equations, the system is discretized by means of the Finite Element Method. In this sense, beam equations are discretized into 2-node linear elements of 12 DOFs (6 by node) whereas the cable equations are discretized into 3-node curved

	$d_c$ [mm]	$m_c$ [kg/m]	$ea_c$ [N]
Guy cables	24.0	2.88	$7.1007 \times 10^7$
Cross Rope	26.0	3.33	$8.3335 \times 10^7$
Insulators	150.0	32.69	$2.7737 \times 10^9$
Conductors	25.9	1.26	$3.5797 \times 10^7$

Table 2: Diameter  $d_c$  and mechanical properties of the cables.

nonlinear elements of 9 DOFs (3 by node). After assembling the matrices, the system equation results:

$$[m] \ddot{\mathbf{u}}(t) + [c] \dot{\mathbf{u}}(t) + [k] \mathbf{u}(t) + \mathbf{k}_{nl}(\mathbf{u}(t)) = \mathbf{f}(t) \quad (2)$$

where  $\mathbf{u}$  is the vector of DOF,  $[m]$ ,  $[c]$  are the mass and damping matrix,  $[k_i]$  is the beam stiffness matrix,  $\mathbf{k}_{nl}(\mathbf{u})$  is the nonlinear vector associated with the cable elements stiffness, and  $\mathbf{f}$  is the vector of external forces.

## 2.2 Damping considerations

**Structural damping.** The structural damping matrix is constructed as a linear combination of the mass and the linearized stiffness matrices  $[c] = \alpha_r[m] + \beta_r[k_l]$ , being  $\alpha_r$  and  $\beta_r$  the respective Rayleigh coefficients. These are computed separately for every structural element based on the corresponding damping ratio, namely  $\epsilon_c = 0.001$  for conductors and guy cables and  $\epsilon_c = 0.005$  for the tower (Gani and Legeron, 2010).

**Aerodynamic damping.** Because of their high flexibility, conductors experience large displacements under the action of wind loads. As a result, the relative motion of the cables with respect to the fluid becomes significant. In this context, the aeroelastic force due to the interaction between the conductor and the wind cannot be disregarded. This force constitutes the aerodynamic damping: it has a resistive effect on the structure dynamics, inducing a reduction in the oscillation amplitude. In this work, the aerodynamic damping is incorporated in the vector of external nodal actions  $\mathbf{f}(t)$  as a dissipative force with opposite sign and same direction as the wind (*i.e.* along the global x-axis):

$$\mathbf{f}_x^{\text{ad}}(t) = -\rho_a c_d a_w \mu_{v_T} \dot{\mathbf{u}}_x(t) \quad (3)$$

being  $\dot{\mathbf{u}}_x(t)$  the vector of instant material velocities along the conductors in the global x-direction,  $\mu_{v_T}$  the mean wind speed,  $\rho_a = 1.225 \text{ kg/m}^3$  the air density,  $c_d = 1$  the drag coefficient for conductors, and  $a_w$  the area of the element exposed to wind.

## 3 STOCHASTIC WIND MODEL

The action of wind on structures depends on the total wind speed  $\mathcal{V}_T(z, t)$ , which is random in nature. However, it can be divided in two parts, the deterministic mean wind speed, which varies with the height  $z$  above the ground, and the turbulent wind part which varies not only with height but also in time:

$$\mathcal{V}_T(z, t) = \mu_{v_T}(z) + \mathcal{V}(z, t) \quad (4)$$

The potential profile of the mean wind speed is  $\mu_{v_T}(z) = v_0(z/10)^\alpha$ . The term  $v_0$  represents the reference wind speed. This parameter depends on the geographical placement of the structure, and is provided by national standards. For terrain category B, the exponent  $\alpha$  assumes the value 0.16 (IEC 60826).

The characterization of the turbulent component, on the other side, is not that straightforward. It is defined by its power spectral density function (PSDF). In the present study, the spectrum proposed by Davenport (1961) is adopted:

$$\frac{s(z, \omega)\omega}{\sigma_v^2} = \frac{2}{3} \frac{f_l(z, \omega)^2}{(1 + f_l(z, \omega)^2)^{4/3}} \quad (5)$$

In this expression,  $s(z, \omega)$  is the PSDF of the along-wind turbulence component,  $\omega$  is the frequency,  $\sigma_v = 6.6$  m/s is the standard deviation of the turbulent wind speed component, and  $f_l(z, \omega) = \omega l_v / \mu_{v_T}(z)$  is a non-dimensional variable which depends on the frequency, the longitudinal integral length of the turbulence  $l_v = 1200$  m, and the mean wind speed. The statistical dependence of the turbulence components at two separate points in the space, due to the spatial dimension of the wind vortices, is defined by the cross spectrum:

$$s^c(z_1, z_2, \omega) = s_{12}^c(\omega) = \sqrt{s(z_1, \omega)s(z_2, \omega)} \exp(-\gamma) \quad (6)$$

$$\gamma = \frac{2\omega[(c_y(y_2 - y_1))^2 + (c_z(z_2 - z_1))^2]^{1/2}}{[\mu_{v_T}(z_1) + \mu_{v_T}(z_2)]} \quad (7)$$

The coherence function  $\gamma$  involves the distance between the pair of discrete points under consideration along the vertical ( $z_2 - z_1$ ) and transverse-to-wind ( $y_2 - y_1$ ) direction, affected by the respective non-dimensional decay coefficients  $c_z=10$  and  $c_y=16$  (Gani and Legeron, 2010).

## 4 RESULTS

### 4.1 Simulation of the stochastic wind load field

The Spectral Representation Method (SRM) (Shinozuka and Jan, 1972) allows to numerically simulate the time-varying turbulent wind speed field. The wind is considered to act transversally to the conductors, in the direction of the x-axis (see Fig. 1). For the sake of brevity, the derivation of the method is not outlined. In this application of the SRM scheme, the random wind speed records  $\mathcal{V}_j(z, t)$   $j = 1, \dots, m$  are generated at  $m = 53$  points on the structure: 13 along the tower height and 20 points along each of both conductors spans placed in the windward yz-plane, as shown in Fig. 2. Since the variation of the wind speed in the along-wind distance between conductors is disregarded, the same wind speed is considered to act in parallel yz-planes. These stochastic processes are simulated as a sum of cosines of random frequencies  $\Omega_n$  and phase angles  $\Phi_{kn}$  :

$$\mathcal{V}_j(z_j, t) = \sum_{k=1}^m \sum_{n=1}^{n_f} |h_{jk}(\omega_n)| \sqrt{2\Delta\omega} \cos[\Omega_n t + \Phi_{kn}] \quad (8)$$

For the simulations, a cutoff frequency of 4 Hz is defined and the spectrum is discretized into  $n_f = 1000$  intervals of amplitude  $\Delta\omega = 0.004$  Hz. Thus, every random frequency is defined as  $\Omega_n = n\Delta\omega + \Psi_{kn}\Delta\omega$ . Both the random parameter  $\Psi_{kn}$  and the independent random phase angles  $\Phi_{kn}$  are uniformly distributed in the interval  $[0, 2\pi]$ . The time step and duration of

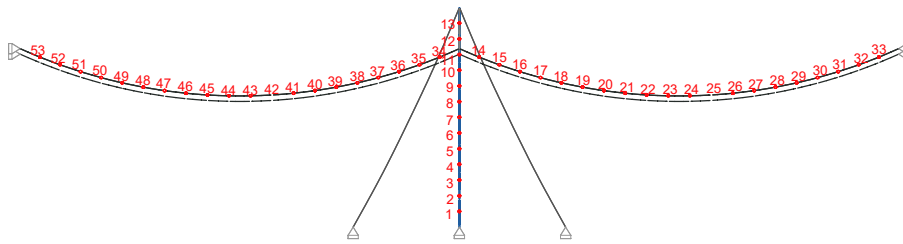


Figure 2: Lateral view (yz-plane) of the CR transmission line. The red dots indicates the discrete points for the generation of the wind load field.

the records are defined as  $dt = 0.125$  s and  $t_f = 340$  s, respectively. The amplitude  $|h_{jk}(\omega_n)|$  corresponds to the  $(j, k)$  entry in the lower triangular matrix  $[h(\omega)]$ , obtained as the Cholesky decomposition of the cross-spectral density matrix  $[s(\omega)]$ .

On this basis, the stochastic wind load field  $\mathcal{F}_j(z, t)$  acting on the tower and conductors is computed as:

$$\mathcal{F}_j(z, t) = \frac{1}{2} \rho_a c_d a_w \mu_{v_T}(z)^2 + \rho_a c_d a_w \mu_{v_T}(z) \mathcal{V}_j(z, t). \tag{9}$$

The drag coefficient  $c_d$  is 1 for conductors and 3.34 for the tower.

In Fig. 3a, a realization of the turbulent wind speed field acting on discrete points along the masts (points  $j = 1-13$ , as already mentioned the same field is applied to both of the CR masts) and along one conductor cable span (points  $j = 14-33$ ) is shown. On the horizontal x-axis,  $j$  identifies the discrete point along the structure (see Fig. 2), whereas in the vertical z-axis the magnitude of the turbulent wind speed at each simulated instant  $t$  (horizontal y-axis) is reported. As expected, the turbulent wind speed oscillates around zero. The plot allows to compare how the wind speed varies at each discrete time along the structure. In effect, within the first 13 points corresponding to the CR tower (see the top-view reported in Fig. 3b) the positive (yellow) and negative (blue) peak values happen at approximately the same time in neighbor points. According to the higher magnitude of exponential decay-coefficient adopted for the global y-axis ( $c_y=16$  whereas  $c_z=10$ ), spatial correlation is weaker along the conductor.

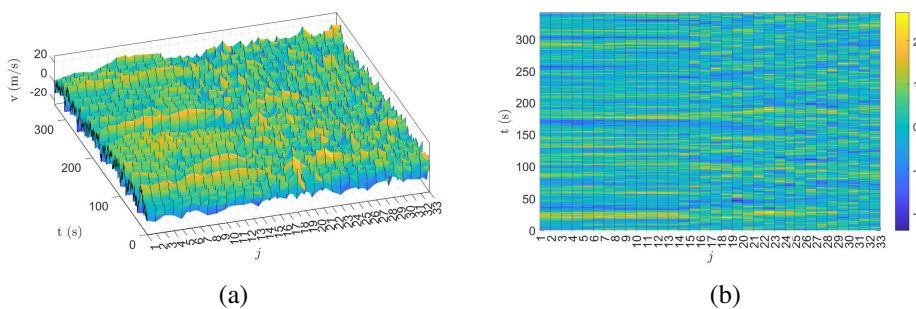


Figure 3: Representation of a particular realization of the wind speed random component at 33 discrete points of the structure.  $j$  identifies the discrete points according to the numbering established in Fig. 2.

## 4.2 Dynamic analysis

Each numerical simulation of the system dynamics consists of two steps. First, the pretension of the guy cables is applied and the static configuration of equilibrium under self weight is computed by means of the nonlinear Newton-Raphson solver. Thus, the initial configuration for

the dynamic analysis of the system under wind load is obtained. The following stage consists on the dynamic analysis of the structure under self weight and the transient wind load field. The static configuration of equilibrium under self weight obtained from step one constitutes the initial conditions for the dynamic study, where the discretized system of equations is integrated by means of a coupled Newmark/Newton-Raphson solver with a fixed time step of  $\Delta t_{dyn} = 0.0625$  s. In order to improve the stability of the dynamic solver, a sine window is applied to the wind load such that its full magnitude be progressively developed during the first 40 s of the simulation. This initial transient period plus the successive 20 seconds are disregarded, and the remaining 5 minutes are analyzed.

The aerodynamic damping has a significant effect on the conductors dynamics. To examine this, an isolated conductor is hung between two supports separated 500 m, placed at 33.4 m above the ground. The conductor sag at the midspan is 22 m, and the material and geometrical properties are the same as reported for the conductors in the CR structure. The isolated conductor is subjected to a wind load field of reference speed  $v_0 = 39$  m/s. In Figure 4, the phase plane corresponding to the along-wind displacements and material velocity of a point placed on the center of the conductor is reported. Figure 4a shows the resulting phase plane when the aerodynamic damping term is not included in the simulation. However, when the aerodynamic damping is accounted for, the phase plane adopts the shape as reported in Fig. 4b. Note that the dissipative condition of the aerodynamic damping provokes radical reductions of the oscillation amplitude and of the maximum positive and negative speed of the material point. Moreover, since it is proportional to the mean wind speed velocity, the effect of aerodynamic

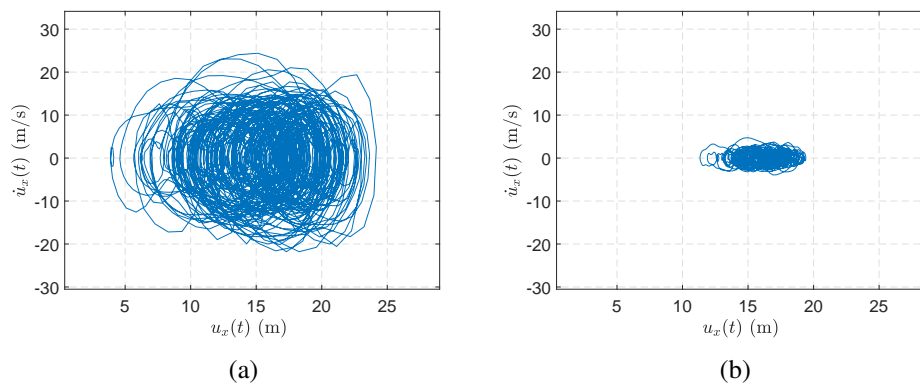


Figure 4: Phase planes associated to a material point placed at the center of the conductor length. (a) Without aerodynamic damping, and (b) with the inclusion of the aerodynamic damping.

damping is expected to be more significant when the reference mean wind speed is higher. Therefore, a parametric sweep is performed varying the reference mean wind speed in the interval  $[1 : 0.5 : 41]$  m/s. As reported in Rango et al. (2018), through Monte Carlo simulations of the problem at hand, and the evaluation of relevant statistics of the structural dynamics (*i.e.* sample mean and standard deviation, cross-correlation, and temporal mean) it can be shown that the stochastic structural response (for instance displacements of the towers and conductors, dynamic tension force on the guy wires) is stationary and ergodic. This implies that, given that the simulation be extended enough in time, the statistical properties of the process can be estimated from a single realization. Therefore, advantage is taken from this feature in order to evaluate the dynamic response as the reference mean wind speed varies. Two particular processes of the structural response are considered: the along-wind (global x-axis) displacements at the center

of the conductor ( $\mathcal{U}_x^c(t)$ ) (point 24 in Fig. 2) and at the top of the leeward CR tower ( $\mathcal{U}_x^t(t)$ ). In Fig. 5 the temporal mean  $\pm$  one standard deviation of each realization of the stochastic processes is reported. As expected, the order of magnitude of the mean displacements at the center of the conductors (Fig. 5a) is much higher than at the top of the tower (Fig. 5b) - in effect, that is the reason for the inclusion of aerodynamic damping on the conductors and not in the CR towers. Naturally, in Fig. 5b both the temporal mean and the amplitude of the envelope rise with the reference mean wind speed. Regarding the displacements on the conductors, the temporal mean rises with the wind speed, however the amplitude of the envelope appears stable from  $v_0 = 20$  m/s approximately, presumably due to the effect of the aerodynamic damping. In

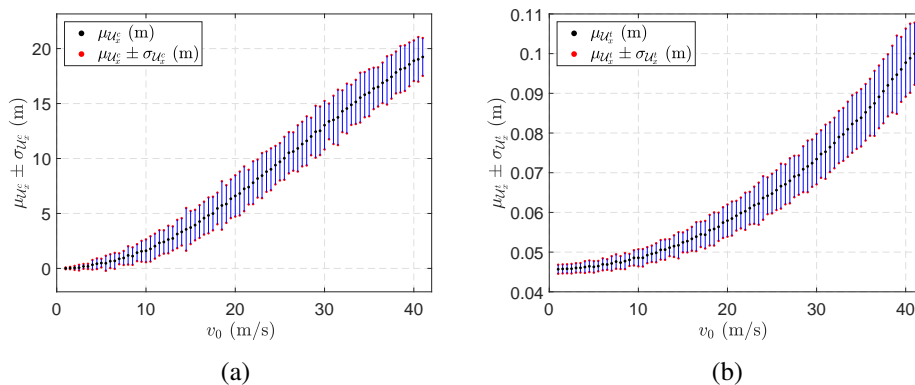


Figure 5: Envelope graph: black dots indicate the temporal mean whereas the red dots represents the mean plus/minus one standard deviation corresponding to the stochastic processes (a)  $\mathcal{U}_x^c(t)$  and (b)  $\mathcal{U}_x^t(t)$ .

order to quantitatively evaluate this trend, the temporal standard deviation is reported in Fig. 6. As noted before, the increment with the wind speed of the standard deviation of the along-wind displacements on the conductor cable is relatively uniform until  $v_0 = 20$  m/s when it becomes erratic. This effect is attributable to the aerodynamic damping: it becomes more relevant when the wind speed rises, inducing the structure to oscillate closer to the mean. This feature has a relevant implication: the highest conductor oscillations not necessarily occurs for the design wind speeds, but will probably be associated to a wide range of velocities below the design one.

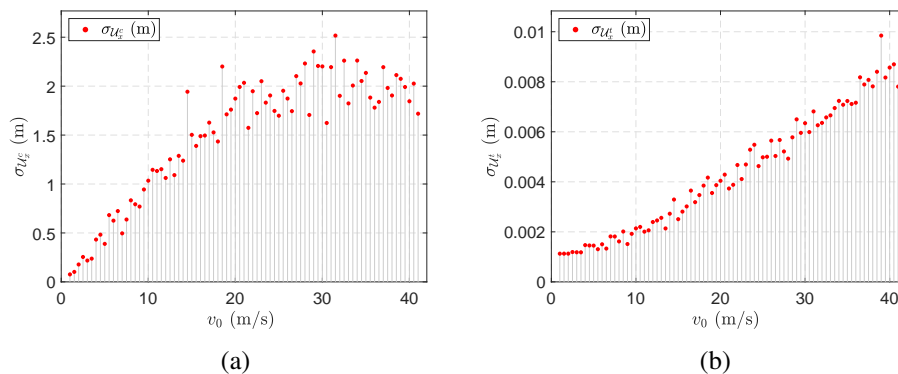


Figure 6: Standard deviation of the stochastic processes (a)  $\mathcal{U}_x^c(t)$  and (b)  $\mathcal{U}_x^t(t)$ .

## 5 CONCLUSIONS

The dynamic behavior of a CR transmission line segment subjected to wind load is evaluated in this work. For this purpose, a mathematical model is stated first. For the computational implementation, the Finite Element Method is adopted as a discretization scheme for the governing nonlinear, partial, differential equations. The cable formulation introduces the geometrical nonlinearities to the system. For the simulation of the spatially correlated temporal wind load fields, the SRM is applied. A particular realization of the stochastic wind field is represented and the spatial correlation along the tower and the conductors is discussed. Moreover, a series of simulation of the dynamic problem are performed in the context of a parametric sweep in which the reference mean wind speed is varied from 1 to 41 m/s. The effect of the aerodynamic damping on the structural dynamic response is studied. It is concluded that the highest oscillations amplitudes on the conductor cables will likely occur for a range of reference wind speeds located below the design wind speed.

## ACKNOWLEDGMENTS

The authors acknowledge the support given by CONICET, MINCyT, and UNS (Argentina) and Faperj, CNPq (Brazil).

## REFERENCES

- Ballaben J., Guzmán A., and Rosales M. Nonlinear dynamics of guyed masts under wind load: Sensitivity to structural parameters and load models. *Journal of Wind Engineering and Industrial Aerodynamics*, 169:128–138, 2017.
- Ballaben J.S. and Rosales M.B. Nonlinear dynamic analysis of a 3d guyed mast. *Nonlinear Dynamics*, 93(3):1395–1405, 2018.
- Davenport A. The spectrum of horizontal gustiness near the ground in high winds. *Quarterly Journal of the Royal Meteorological Society*, 87(372):194–211, 1961.
- Fleck Fadel Miguel L., Fleck Fadel Miguel L., Riera J., Kaminski J., and Ramos de Menezes J. Assessment of code recommendations through simulation of EPS wind loads along a segment of a transmission line. *Engineering Structures*, 43:1–11, 2012.
- Gani F. and Legeron F. Dynamic response of transmission lines guyed towers under wind loading. *Canadian Journal of Civil Engineering*, 37:450–464, 2010.
- Guzmán A.M., Rosales M.B., and Filipich C.P. Natural vibrations and buckling of a spatial lattice structure using a continuous model derived from an energy approach. *International Journal of Steel Structures*, 17(2):565–578, 2017.
- Hamada A., King J., El Damatty A., Bitsuamlak G., and Hamada M. The response of a guyed transmission line system to boundary layer wind. *Engineering Structures*, 139:135–152, 2017.
- IEC 60826. Design Criteria of Overhead Transmission Lines. International standard, International Electrotechnical Commission (IEC), Geneva, Switzerland, 2003.
- Luongo A., Rega G., and Vestroni F. Planar non-linear free vibrations of an elastic cable. *International Journal of Non-Linear Mechanics*, 19(1):39–52, 1984.
- Rango B., Ballaben J., Sampaio R., and Rosales M. Uncertainty quantification in a transmission line guyed tower under wind load. *Proceedings of the ICVRAM-ISUMA UNCERTAINTIES 2018, Florianopolis, Brazil*, 2018.
- Shinozuka M. and Jan C. Digital simulation of random processes and its applications. *Journal of Sound and Vibration*, 25(1):111–128, 1972.